WEP Warwick Evans Publishing

International Journal of Mechanical and Electrical Engineering

ISSN: 3005-9615 (Print), ISSN: 3005-7132 (Online)
Volume 8, Number 6, Year 2026
DOI: https://doi.org/10.62051/ijmee.v8n6.04

Comparison of Electric-Field Distributions Above Conventional and Early Streamer Emission Lightning Rods Under Thunderstorm Electric Fields

Bin Hu [1,*], Shifan Shan [2] and Jiajia Pan [1]

[1] China Electric Power Research Institute, Beijing, 100192, China

[2] School of Electrical Engineering and Automation, Hefei University of Technology, Hefei, Anhui, 230009, China

* Corresponding author: Bin Hu (Email: hb19165520886@126.com)

ABSTRACT

The electric field above a lightning-rod tip is an important parameter for evaluating its lightning-interception performance. In this study, two-dimensional axisymmetric electrostatic models of a conventional lightning rod and an ESE lightning rod were established using the finite-element method. The electric-field distributions within 2 m above the rod tips were calculated under different thunderstorm background electric fields and installation heights. The results showed that the electric field decreased rapidly with distance from the tip and increased with both background electric field and installation height. Under the same conditions, the electric field above the ESE lightning rod was higher than that above the conventional lightning rod, particularly in the near-tip region. The electric-field difference above the ESE and conventional lightning rods increased with increasing background electric field, while its sensitivity to installation height gradually decreased at greater installation heights. These results provide a quantitative basis for comparing the electric-field enhancement characteristics of conventional and ESE lightning rods.

KEYWORDS

Lightning Rod; Early Streamer Emission; Electric-field Distribution; Thunderstorm Background Electric Field; Finite-element Calculation.

1. INTRODUCTION

Lightning attachment to a grounded lightning rod is controlled by the electric-field enhancement produced near its tip under thunderstorm conditions [1]. As a downward lightning leader approaches the ground, the electric field around a grounded lightning rod increases, leading first to streamer development and, under sufficiently strong electrical conditions, to the inception of a stable upward connecting leader [2,3]. The initiation and subsequent propagation of this upward leader are key processes determining whether the lightning rod participates in the final lightning attachment [4]. Therefore, the electric field above the lightning-rod tip is an important parameter for evaluating its lightning-interception capability [5]. Because the local field enhancement is strongly affected by the geometry and installation height of the lightning rod [6], quantitatively evaluating the electric-field distribution above different types of lightning rods is important for understanding their lightning-interception characteristics.

Existing studies of lightning attachment to grounded structures generally begin by calculating the electric-field or background-potential distribution around the structure [7,8]. The calculated field distribution is then used to evaluate streamer inception, streamer-to-leader transition, and the

Content from this work may be used under the terms of CC BY-NC 4.0 licence (https://creativecommons.org/licenses/by-nc/4.0/).
Published by Warwick Evans Publishing.

inception and propagation of a stable upward connecting leader, followed by the final interaction between the upward connecting leader and the descending leader [9,10]. Various physical models, including the critical-streamer-length concept, generalized leader-inception models, and self-consistent leader inception and propagation models, have been developed following this approach [11-14]. These studies have demonstrated that the local electric field around the tip of a grounded object plays a fundamental role in the lightning attachment process. Comparative studies of conventional Franklin rods and early streamer emission (ESE) lightning rods have also been reported [15-17]; however, the claimed improvement in lightning-interception performance of ESE lightning rods remains under discussion [18-20]. In particular, quantitative information on the differences in the spatial electric-field distributions above conventional and ESE lightning rods under different thunderstorm background fields, and on how these differences vary with installation height, remains limited.

In this study, two-dimensional axisymmetric electrostatic models of a conventional lightning rod and an ESE6000 early streamer emission lightning rod were established. The axial electric-field distributions within 2 m above the lightning-rod tips were calculated under different cloud-to-ground background electric fields and different installation heights. The effects of background electric field and installation height on the electric-field enhancement of the two lightning rods were compared, and the differences in their electric-field distributions above the tips were quantitatively evaluated.

2. METHODS

2.1. Calculation of Electric Field above Lightning Rod

To calculate the electric field above the conventional and ESE lightning rods under a prescribed thunderstorm background electric field, the lightning rod-ground system was treated as an electrostatic problem. Under this approximation, time-varying electromagnetic effects were neglected, and the governing relations in the air domain are

$$D = \varepsilon_0 \varepsilon_r E, \nabla \cdot D = \rho_v, \nabla \times E = 0 \tag{1}$$

where D is the electric displacement vector, E is the electric-field vector, ρ_v is the free charge density, ε_0 is the vacuum permittivity, and ε_r is the relative permittivity.

Because the electrostatic field is irrotational, a scalar electric potential V can be introduced as

$$E = -\nabla V \tag{2}$$

Substituting (2) into Gauss's law gives the governing equation for the electric potential,

$$\nabla \cdot (\varepsilon_0 \varepsilon_r \nabla V) = -\rho_v \tag{3}$$

In the present electrostatic model, free space charge in the air domain was neglected. Since the air was assumed to be homogeneous with $\varepsilon_r = 1$, (3) reduces to the Laplace equation,

$$\nabla^2 V = 0 \tag{4}$$

The electric-potential distribution was obtained by solving (4), and the electric field was then calculated from (2). The axial electric-field distribution within 2 m above each lightning-rod tip was extracted for comparison under different thunderstorm background electric fields and installation heights.

2.2. Two-dimensional Axisymmetric Electrostatic Model of Lightning Rod

A finite-element solver was adopted to solve the Laplace equation, and the electric-field distribution above the lightning rods was obtained. The modeling objects included the conventional lightning rod and the ESE lightning rod shown in Figs. 1(a) and 1(b), respectively. The geometry of the ESE lightning rod was designed to resemble that of the Duval-Messien SATELIT®+G2 6000 early streamer emission lightning rod [21].

As shown in Figs. 1(b) and 1(c), a closed region of 2000 m × 2000 m containing the lightning rod was selected as the computational domain, and appropriate boundary conditions were imposed. The bottom boundary of the computational domain and the lightning rod were both set to a potential of 0 V. Considering that the thundercloud-to-ground gap was approximated by a uniform background electric field [22], a potential corresponding to the thundercloud potential was applied to the top boundary of the computational domain to establish the prescribed background electric field across the gap. All the remaining outer boundaries were defined as Neumann boundaries $\vec{n} \cdot \vec{D} = 0$.

During the calculation, the lightning rod was subtracted from the computational domain, and the relative permittivity of the remaining region was set to 1. As shown in Figs. 1(c) and 1(f), local mesh refinement was implemented around the lightning rod to improve the calculation accuracy of the electric field above the lightning rod.

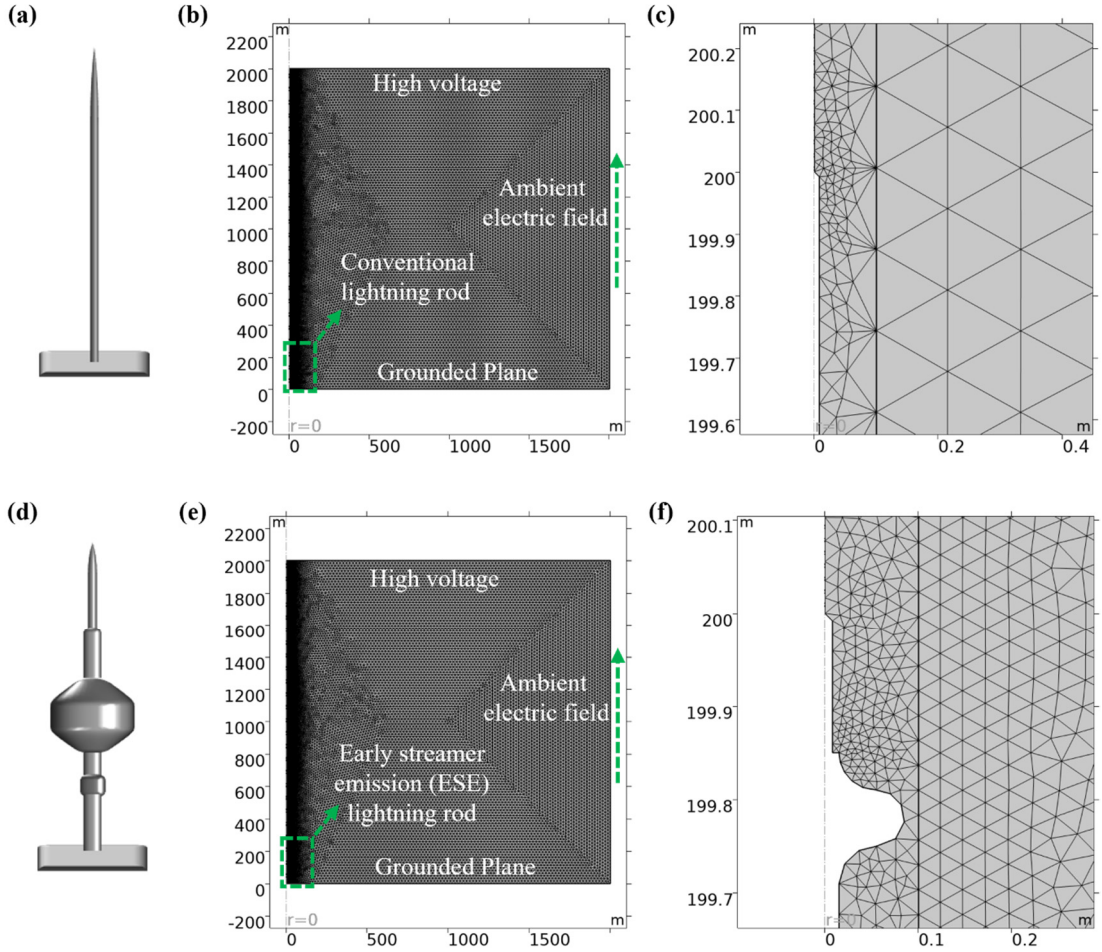


Fig 1. (a) Two-dimensional axisymmetric electrostatic models of the conventional and ESE lightning rods: (a) geometry of the conventional lightning rod; (b) computational domain and boundary conditions for the conventional lightning rod; (c) enlarged view of the region around the conventional lightning rod in (b); (d) geometry of the ESE lightning rod; (e) computational domain and boundary conditions for the ESE lightning rod; (f) enlarged view of the region around the ESE lightning rod in (d).

3. RESULTS

Figure 2 shows the electric-field distributions around the conventional and ESE lightning rods under a thunderstorm background electric field of 10 kV/m and an installation height of 200 m. For both lightning rods, the electric field over most of the computational domain remained close to the background level, whereas a pronounced field enhancement occurred in the vicinity of the lightning-rod tip. The enlarged views in Figs. 2(b) and 2(d) further showed that the electric field decreased rapidly with increasing distance from the rod surface. For the conventional lightning rod, the high-field region was mainly concentrated around the pointed tip, while the ESE lightning rod exhibited a more complex local field distribution because of its different geometric configuration, with field enhancement occurring not only near the upper tip but also around the surrounding metallic structure. Farther away from the lightning rods, the influence of their geometries gradually weakened, and the electric field approached the background value.

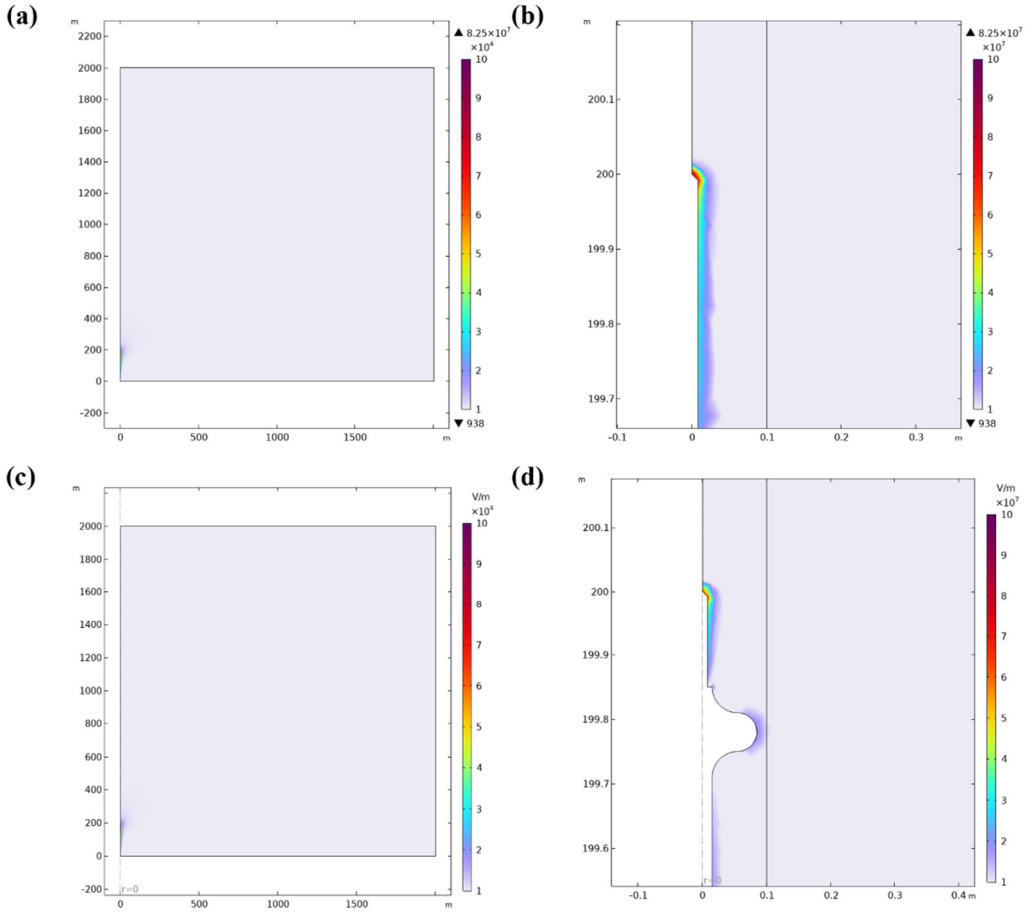


Fig 2. (a) Electric-field distribution above the conventional lightning rod under a thunderstorm background electric field of 10 kV/m and an installation height of 200 m; (b) Enlarged view of the region around the lightning rod in (a); (c) Electric-field distribution above the ESE lightning rod under a thunderstorm background electric field of 10 kV/m and an installation height of 200 m; (d) Enlarged view of the region around the ESE lightning rod in (c).

The axial electric-field distributions within 2 m above the conventional and ESE lightning-rod tips under different thunderstorm background electric fields were compared in Figure 3. As shown in Fig. 3(a), for both lightning rods, the electric field reached its maximum near the tip and decreased rapidly with increasing distance from the tip, with the most pronounced decay occurring within the near-tip region. Increasing the thunderstorm background electric field increased the electric-field strength above both lightning rods. Under the same background electric field, the electric field above the ESE

lightning rod was higher than that above the conventional lightning rod, particularly close to the tip. Figure 3(b) further showed that the electric-field difference between the two lightning rods increased with increasing background electric field, while it decreased sharply with distance from the tip and became relatively small farther away. These results indicated that the difference in field enhancement between the ESE and conventional lightning rods was mainly concentrated in the immediate vicinity of the lightning-rod tip and became more pronounced under stronger thunderstorm background electric fields.

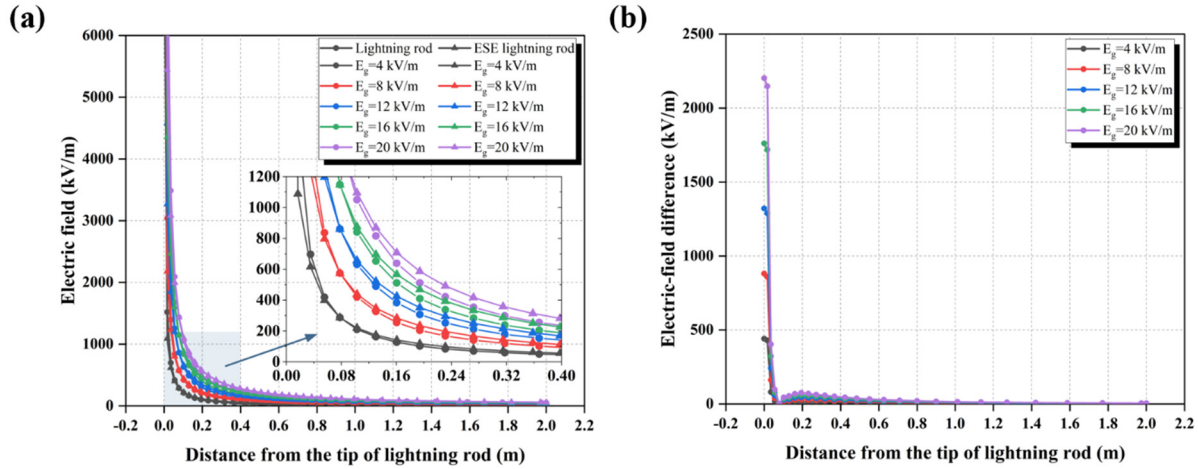


Fig 3. Electric-field distributions within 2 m above the conventional and ESE lightning rods under different thunderstorm background electric fields at an installation height of 50 m; (b) electric-field difference between the ESE and conventional lightning rods under different background electric fields, calculated by subtracting the field above the conventional lightning rod from that above the ESE lightning rod in (a)

Figure 4 compares the axial electric-field distributions within 2 m above the conventional and ESE lightning-rod tips at different installation heights under a thunderstorm background electric field of 10 kV/m. As shown in Fig. 4(a), the electric field above both lightning rods increased with increasing installation height and decreased rapidly with increasing distance from the tip. At the same installation height, the electric field above the ESE lightning rod remained higher than that above the conventional lightning rod, particularly in the near-tip region. Figure 4(b) further showed that the electric-field difference between the two lightning rods increased with installation height, but the rate of increase gradually decreased. At the rod tip, the electric-field difference increased from approximately 1100 kV/m at an installation height of 50 m to approximately 2400 kV/m at 100 m, corresponding to an increase of about 1300 kV/m. In contrast, when the installation height was further increased from 100 to 250 m, the tip electric-field difference increased only from approximately 2400 to 3000 kV/m, an increase of about 600 kV/m. This result indicated that the influence of installation height on the difference in field enhancement between the ESE and conventional lightning rods became progressively weaker at greater installation heights. Moreover, the electric-field difference decreased rapidly with distance from the tip and became relatively small farther away from the lightning rods.

4. CONCLUSION

The electric-field distribution above a lightning rod is closely related to its lightning-interception process. In this study, the electric fields above conventional and ESE lightning rods were compared under different thunderstorm background electric fields and installation heights. The electric field

above both lightning rods decreased rapidly with distance from the tip and increased with increasing background electric field and installation height. Under the same conditions, the ESE lightning rod produced a stronger near-tip electric field than the conventional lightning rod. The difference between the two rods increased with background electric field, whereas the additional increase in this difference became smaller as the installation height increased. Overall, the differences between the two lightning rods were mainly concentrated in the near-tip region.

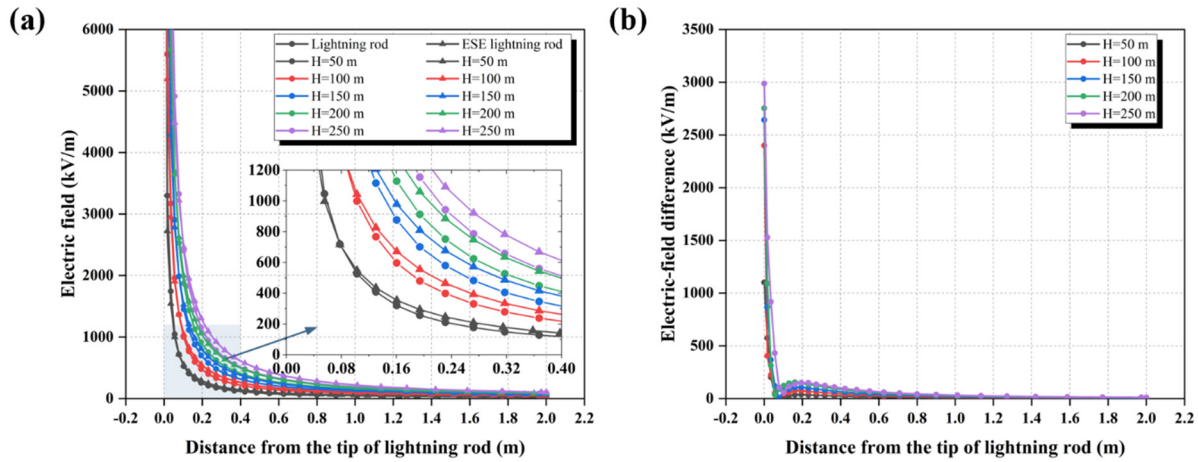


Fig 4. Electric-field distributions within 2 m above the conventional and ESE lightning rods at different installation heights under a thunderstorm background electric field of 10 kV/m; (b) electric-field difference between the ESE and conventional lightning rods under different installation heights, calculated by subtracting the field above the conventional lightning rod from that above the ESE lightning rod in (a).

REFERENCES

[1] Bazelyan, E. M., Raizer, Y. P., & Aleksandrov, N. L. (2008). Corona initiated from grounded objects under thunderstorm conditions and its influence on lightning attachment. Plasma Sources Science and Technology, 17(2), 024015. https://doi.org/10.1088/0963-0252/17/2/024015.

[2] Becerra, M., & Cooray, V. (2006). Time dependent evaluation of the lightning upward connecting leader inception. Journal of Physics D: Applied Physics, 39(21), 4695-4702. https://doi.org/10.1088/0022-3727/39/21/022.

[3] Lalande, P., Bondiou-Clergerie, A., Bacchiega, G., & Gallimberti, I. (2002). Observations and modeling of lightning leaders. Comptes Rendus Physique, 3(10), 1375-1392. https://doi.org/10.1016/s1631-0705(02)01410-1.

[4] Saba, M. M. F., & et al. (2023). Upward leaders initiated from instrumented lightning rods during the approach of a downward leader in a cloud-to-ground flash. Journal of Geophysical Research: Atmospheres, 128, e2022JD038082. https://doi.org/10.1029/2022jd038082.

[5] Shostak, V., Petrenko, T., Janischewskyj, W., & Rachidi, F. (2012). Electric field within lightning protection volume in presence of a descending leader. Electric Power Systems Research, 85, 82-89. https://doi.org/10. 1016/ j. epsr. 2011. 11.010.

[6] Aleksandrov, N. L., Bazelyan, E. M., D'Alessandro, F., & Raizer, Y. P. (2005). Dependence of lightning rod efficacy on its geometric dimensions—a computer simulation. Journal of Physics D: Applied Physics, 38(8), 1225-1238. https://doi.org/10.1088/0022-3727/38/8/014.

[7] Dellera, L., & Garbagnati, E. (1990). Lightning stroke simulation by means of the leader progression model. I. Description of the model and evaluation of exposure of free-standing structures. IEEE Transactions on Power Delivery, 5(4), 2009-2022. https://doi.org/10.1109/61.103684.

[8] Petrov, N. I., & Waters, R. T. (1995). Determination of the striking distance of lightning to earthed structures. Proceedings of the Royal Society A: Mathematical, Physical and Engineering Sciences, 450(1940), 589-601. https://doi.org/10.1098/rspa.1995.0105.

[9] Rizk, F. A. M. (2009). Modeling of lightning exposure of buildings and massive structures. IEEE Transactions on Power Delivery, 24(4), 1987-1998. https://doi.org/10.1109/tpwrd.2009.2028791.

[10] Cooray, V., & Becerra, M. (2012). Attractive radii of vertical and horizontal conductors evaluated using a self consistent leader inception and propagation model—SLIM. Atmospheric Research, 117, 64-70. https://doi.org/ 10. 1016/ j. atmosres.2012.05.008.

[11] Akyuz, M., & Cooray, V. (2001). The Franklin lightning conductor: Conditions necessary for the initiation of a connecting leader. Journal of Electrostatics, 51-52, 319-325. https://doi.org/10.1016/s0304-3886(01)00144-4.

[12] Rizk, F. A. M. (1990). Modeling of transmission line exposure to direct lightning strokes. IEEE Transactions on Power Delivery, 5(4), 1983-1997. https://doi.org/10.1109/61.103683.

[13] Becerra, M., & Cooray, V. (2006). A simplified physical model to determine the lightning upward connecting leader inception. IEEE Transactions on Power Delivery, 21(2), 897-908. https://doi.org/10.1109/tpwrd.2005.858769.

[14] Becerra, M., & Cooray, V. (2006). A self-consistent upward leader propagation model. Journal of Physics D: Applied Physics, 39(16), 3708-3715. https://doi.org/10.1088/0022-3727/39/16/023.

[15] Allen, N. L., Cornick, K. J., Faircloth, D. C., & Kouzis, C. M. (1998). Tests of the 'early streamer emission' principle for protection against lightning. IEE Proceedings—Science, Measurement and Technology, 145(5), 200-206. https://doi.org/10.1049/ip-smt:19982109.

[16] Pecastaing, L., Reess, T., de Ferron, A., Souakri, S., Smycz, E., Skopec, A., & Stec, C. (2015). Experimental demonstration of the effectiveness of an early streamer emission air terminal versus a Franklin rod. IEEE Transactions on Dielectrics and Electrical Insulation, 22(2), 789-798. https://doi.org/10.1109/tdei.2014.004712.

[17] Ozdemir, A., & Ilhan, S. (2023). Experimental performance analysis of conventional and non-conventional lightning protection systems—Preliminary results. Electric Power Systems Research, 216, 109080. https://doi.org/ 10. 1016/ j. epsr.2022.109080.

[18] Van Brunt, R. J., Nelson, T. L., & Stricklett, K. L. (2000). Early streamer emission lightning protection systems: An overview. IEEE Electrical Insulation Magazine, 16(1), 5-24. https://doi.org/10.1109/57.814846.

[19] Uman, M. A., & Rakov, V. A. (2002). A critical review of nonconventional approaches to lightning protection. Bulletin of the American Meteorological Society, 83(12), 1809-1820. https://doi.org/10.1175/bams-83-12-1809.

[20] Cooray, V. (2018). The similarity of the action of Franklin and ESE lightning rods under natural conditions. Atmosphere, 9(6), 225. https://doi.org/10.3390/atmos9060225.

[21] Duval Messien. (n.d.). Your solution against lightning: SATELIT®+G2 Early Streamer Emission System [Report]. Duval Messien.

[22] Cooray, V., Rakov, V. A., & Theethayi, N. (2007). The lightning striking distance—Revisited. Journal of Electrostatics, 65(5-6), 296-306. https://doi.org/10.1016/j.elstat.2006.09.001.